arXiv:1611.06490v1 [math.NA] 20 Nov 2016

Computational modeling of magnetic hysteresis with thermal effects

Martin Kružík [*], Jan Valdman [†]

November 22, 2016

Abstract

We study computational behavior of a mesoscopic model describing temperature/external magnetic field-driven evolution of magnetization. Due to nonconvex anisotropy energy describing magnetic properties of a body, magnetization can develop fast spatial oscillations creating complicated microstructures. These microstructures are encoded in Young measures, their first moments then identify macroscopic magnetization. Our model assumes that changes of magnetization can contribute to dissipation and, consequently, to variations of the body temperature affecting the length of magnetization vectors. In the ferromagnetic state, minima of the anisotropic energy density depend on temperature and they tend to zero as we approach the so-called Curie temperature. This brings the specimen to a paramagnetic state. Such a thermo-magnetic model is fully discretized and tested on two-dimensional examples. Computational results qualitatively agree with experimental observations. The own MATLAB code used in our simulations is available for download.

Keywords: dissipative processes, hysteresis, micromagnetics, numerical solution, Young measures

1 Introduction

In the isothermal situation, the configuration of a rigid ferromagnetic body occupying a bounded domain $\Omega \subset \mathbb{R}^d$ is usually described by a magnetization $m : \Omega \to \mathbb{R}^d$ which denotes density of magnetic spins and which vanishes if the temperature θ is above the so-called Curie temperature θ_c. Brown [5] developed a theory called "micromagnetics" relying on the assumption that equilibrium states of saturated ferromagnets are minima of an energy functional. This variational theory is also capable of predictions of formation of domain microstructures. We refer e.g. to [15] for a survey on the topic. Starting from a microscopic description of the magnetic energy we will continue to a mesoscopic level which is convenient for analysis of magnetic microstructures.

On microscopic level, the magnetic Gibbs energy consists of several contributions, namely an anisotropy energy $\int_\Omega \psi(m,\theta)\,\mathrm{d}x$, where ψ is the-so called anisotropy energy density describing crystallographic properties of the material, an exchange energy $\frac{1}{2}\int_\Omega \varepsilon|\nabla m(x)|^2\mathrm{d}x$ penalizing spatial changes of the magnetization, the non-local magnetostatic energy $\frac{1}{2}\int_{\mathbb{R}^d}\mu_0|\nabla u_m(x)|^2\mathrm{d}x$, work done by an external magnetic field h which reads $-\int_\Omega h(x)\cdot m(x)\,\mathrm{d}x$, and a calorimetric term $\int_\Omega \psi_0\,\mathrm{d}x$. The anisotropic energy density depends on the material properties and defines the so-called easy axes of the material, i.e., lines along which the smallest external field is needed to magnetize fully the specimen. There are three types of anisotropy: uniaxial, triaxial, and cubic. Furthermore, ψ is supposed to be a nonnegative function, even in its first variable, i.e., $\pm m$ are assigned the same anisotropic energy. In the magnetostatic energy, u_m is the magnetostatic potential related to m by the Poisson problem $\mathrm{div}(\mu_0\nabla u_m - \chi_\Omega m) = 0$ arising from Maxwell equations. Here $\chi_\Omega : \mathbb{R}^d \to \{0,1\}$ denotes the characteristic function of Ω and $\mu_0 = 4\pi \times 10^{-7}\mathrm{N/A}^2$ is the permeability of vacuum.

[*]Institute of Information Theory and Automation of the CAS, Pod vodárenskou věží 4, CZ-182 08 Praha 8, Czech Republic

[†]Institute of Mathematics and Biomathematics, Faculty of Science, University of South Bohemia, Branišovská 31, CZ–37005, Czech Republic and Institute of Information Theory and Automation, Academy of Sciences, Pod vodárenskou věží 4, CZ–18208 Praha 8, Czech Republic.

A widely used model describing steady-state isothermal configurations is due to Landau and Lifshitz [18, 19] (see also e.g. Brown [5] or Hubert and Schäfer [11]), relying on minimization of Gibbs' energy with θ as a fixed parameter, i.e.,

$$\left.\begin{array}{ll} \text{minimize} & G_\varepsilon(m) := \displaystyle\int_\Omega \Big(\psi(m,\theta) + \frac{1}{2} m\cdot\nabla u_m + \frac{\varepsilon}{2}|\nabla m|^2 - h\cdot m \,\mathrm{d}x\Big)\,\mathrm{d}x \\ \text{subject to} & \operatorname{div}(\mu_0 \nabla u_m - \chi_\Omega m) = 0 \ \text{ in } \mathbb{R}^d\,, \\ & m \in H^1(\Omega;\mathbb{R}^d), \quad u_m \in H^1(\mathbb{R}^d), \end{array}\right\} \tag{1}$$

where the anisotropy energy ψ is considered in the form

$$\psi(m,\theta) := \phi(m) + a_0(\theta - \theta_{\mathrm{c}})|m|^2 - \psi_0(\theta), \tag{2}$$

where a_0 determines the intensity of the thermo-magnetic coupling. To see a paramagnetic state above Curie temperature θ_{c}, one should consider $a_0 > 0$. The isothermal part of the anisotropy energy density $\phi : \mathbb{R}^d \to [0,\infty)$ typically consists of two components $\phi(m) = \phi_{\mathrm{poles}}(m) + b_0|m|^4$, where $\phi_{\mathrm{poles}}(m)$ is chosen in such a way to attain its minimum value (typically zero) precisely on lines $\{ts_\alpha;\ t \in \mathbb{R}\}$, where each $s_\alpha \in \mathbb{R}^d$, $|s_\alpha| = 1$ determines an axis of easy magnetization. Typical examples are $\alpha = 1$ for uni-axial, $1 \le \alpha \le 3$ for triaxial, and $1 \le \alpha \le 4$ for cubic magnets. We can consider a uniaxial magnet with $\phi_{\mathrm{poles}}(m) = \sum_{i=1}^{d-1} m_i^2$, for instance. Here, the easy axis coincides with the d-th axis of the Cartesian coordinate system, i.e., $s_\alpha := (0,\dots,1)$. On the other hand, $b_0|m|^4$ is used to ensure that, for $\theta < \theta_{\mathrm{c}}$, $\psi(\cdot,\theta)$ is minimized at ts_α for $|t|^2 = (\theta_{\mathrm{c}} - \theta)a_0/(2b_0)$ and that $\psi(\cdot,\theta)$ is coercive. Such energy has already been used in [25]. For $\varepsilon > 0$, the exchange energy $\varepsilon|\nabla m|^2$ guarantees that the problem (1) has a solution m_ε. Zero-temperature limits of this model consider, in addition, that the minimizers to (1) are constrained to be valued on the sphere with the radius $\sqrt{a_0\theta_{\mathrm{c}}/(2b_0)}$ and were investigated, e.g., by Choksi and Kohn [8], DeSimone [9], James and Kinderlehrer [12], James and Müller [13], Pedregal [22, 23], Pedregal and Yan [24] and many others.

In [3], the authors first consider a mesoscopic micromagnetic energy arising for setting $\varepsilon := 0$ in (1). Moreover, it is assumed that changes of magnetization cause dissipation which is transformed into heat. Increasing temperature of the specimen influences its magnetic properties. Therefore, they analyze an evolutionary anisothermal mesoscopic model of a magnetic material. The aim of this paper is to discretize this model in space and time, and to perform numerical experiments. The plan of our work is as follows. In Section 2 we describe the stationary mesoscopic model. The evolutionary problem is introduced in Section 3. Section 4 provides us with a numerical approximation and some computational experiments. We finally conclude with a few remarks in Section 5. An appendix then briefly introduces an important tool for the analysis as well as for numerics, namely Young measures.

2 Mesoscopic description of magnetization

For ε small, minimizers m_ε of (1) typically exhibit fast spatial oscillations, usually called microstructure. Indeed, the anisotropy energy, which forces magnetization vectors to be aligned with the easy axis (axes), competes with the magnetostatic energy preferring divergence-free magnetization fields. It was shown in [9] by a scaling argument that for large domains Ω the exchange energy contributions becomes less and less significant in comparison with other terms and thus the so-called "no-exchange" formulation is a justified approximation. This generically leads, however, to nonexistence of a minimum for uniaxial ferromagnets as shown in [12] without an external field h. Hence, various ways to extend the notion of a solution were developed. The idea is to capture the limiting behavior of minimizing sequences of $G_\varepsilon(m)$ as $\varepsilon \to 0$. This leads to a "relaxed problem" (3) involving possibly so-called Young measures ν's [32] which describe fast spatial changes of the magnetization and can capture limit patterns.

It can be proved [9, 22] that this limit configuration (ν, u_m) solves the following minimization problem

involving temperature as a parameter and a "mesoscopic" Gibbs' energy G:

$$\left.\begin{array}{lll} \text{minimize} & G(\nu,m) := \displaystyle\int_\Omega \big(\psi \bullet \nu + \frac{1}{2} m{\cdot}\nabla u_m - h{\cdot}m\big)\,\mathrm{d}x & \\ \text{subject to} & \mathrm{div}\big(\mu_0 \nabla u_m - \chi_\Omega m\big) = 0 & \text{on } \mathbb{R}^d, \\ & m = \mathrm{id} \bullet \nu & \text{on } \Omega, \\ & \nu \in \mathscr{Y}^p(\Omega;\mathbb{R}^d), \quad m \in L^p(\Omega;\mathbb{R}^d), \quad u_m \in H^1(\mathbb{R}^d)\ , & \end{array}\right\} \tag{3}$$

where the "momentum" operator " $\bullet$ " is defined by $[\psi \bullet \nu](x) := \int_{\mathbb{R}^d} \psi(s,\theta)\nu_x(\mathrm{d}s)$ and similarly for $\mathrm{id} : \mathbb{R}^d \to \mathbb{R}^d$ which denotes the identity and $\nu \in \mathscr{Y}^p(\Omega;\mathbb{R}^d)$. Here, the set of Young measures $\mathscr{Y}^p(\Omega;\mathbb{R}^d)$ can be viewed as a collection of probability measures $\nu = \{\nu_x\}_{x\in\Omega}$ such that ν_x is a probability measure on $\mathbb{R}^d$ for almost every $x \in \Omega$. It means that ν_x is a positive Radon measure such that $\nu_x(\mathbb{R}^d) = 1$. We refer to Appendix for more details on Young measures.

In [3], the authors built and analyzed a mesoscopic model in anisothermal situations. A closely related thermodynamically consistent model on the microscopic level was previously introduced in [25] to model a ferro/para magnetic transition. Another related microscopic model with a prescribed temperature field was investigated in [2]. The goal of this contribution is to discretize the model from [3] and test it on computational examples. In order to make our exposition reasonably self-content, we closely follow the derivation of the model presented in [3]. We also point out that computationally efficient numerical implementation of isothermal models can be found in [6, 14, 16, 17], where such a model was used in the isothermal variant.

In what follows we use a standard notation for Sobolev, Lebesgue spaces and the space of continuous functions. We denote by $C_0(\mathbb{R}^d)$ the space of continuous functions $\mathbb{R}^d \to \mathbb{R}$ vanishing at infinity. Further, $C_p(\mathbb{R}^d) := \{f \in C(\mathbb{R}^d);\ f/(1+|\cdot|^p) \in C_0(\mathbb{R}^d)\}$, and $C^p(\mathbb{R}^d) := \{f \in C(\mathbb{R}^d);\ |f|/(1+|\cdot|^p) \le C,\ C>0\}$.

3 Evolution problem and dissipation

If the external magnetic field h varies during a time interval $[0,T]$ with a horizon $T > 0$, the energy of the system and magnetic states evolve, as well. Changes of the magnetization may cause energy dissipation. As the magnetization is the first moment of the Young measure, ν, we relate the dissipation on the mesoscopic level to temporal variations of some moments of ν and consider these moments as separate variables. This approach was already used in micromagnetics in [28, 29] and proved to be useful also in modeling of dissipation in shape memory materials, see e.g. [21]. In view of (2), we restrict ourselves to the first two moments defining $\lambda = (\lambda_1, \lambda_2) \subset \mathbb{R}^d \times \mathbb{R} = \mathbb{R}^{d+1}$ giving rise to the constraint

$$\lambda = L \bullet \nu\ , \qquad \text{where}\ \ L(m) := (m, |m|^2) \tag{4}$$

and consider the specific dissipation potential depending on a "yield set" $S \subset \mathbb{R}^{d+1}$

$$\zeta(\dot\lambda) := \delta_S^*(\dot\lambda) + \frac{\epsilon}{q}|\dot\lambda|^q, \qquad q \ge 2, \tag{5}$$

The set S determines activation threshold for the evolution of λ. It is a convex compact set containing zero in its interior. The function $\delta_S^* \ge 0$ is the Fenchel conjugate of the indicator function of S. Consequently, it is convex and degree-1 positively homogeneous with $\delta_S^*(0) = 0$. In fact, the first term describes purely hysteretic losses, which are rate-independent and which we consider dominant, and the second term models rate-dependent dissipation.

In view of (2)–(3), the specific mesoscopic Gibbs free energy, expressed in terms of ν, λ and θ, reads as

$$g(t,\nu,\lambda,\theta) := \phi \bullet \nu + (\theta - \theta_\mathrm{c})\vec{a}{\cdot}\lambda - \psi_0(\theta) + \frac{1}{2} m{\cdot}\nabla u_m - h(t){\cdot}m \tag{6a}$$

$$\text{with}\ \ m = \mathrm{id} \bullet \nu \tag{6b}$$

where we denoted $\vec{a} := (0, \dots, 0, a_0)$ with a_0 from (2) and, of course, u_m again from (1), which makes g non-local.

As done already in [3], we relax the constraint (4) by augmenting the total Gibbs free energy (i.e., ψ integrated over Ω) by the term $\frac{\varkappa}{2}\|\lambda - L \bullet \nu\|^2_{H^{-1}(\Omega;\mathbb{R}^{d+1})}$ with (presumably large) $\varkappa \in \mathbb{R}^+$ and with $H^{-1}(\Omega) \cong H^1_0(\Omega)^*$. Thus, λ's no longer exactly represent the "macroscopic" momenta of the magnetization but rather are in a position of a phase field or an internal parameter of the model. We define the mesoscopic Gibbs free energy $\mathscr{G}$ as

$$\mathscr{G}(t, \nu, \lambda, \theta) := \int_\Omega \Big(g(t, \nu, \lambda, \theta) + \frac{\varkappa}{2} |\nabla \Delta^{-1}(\lambda - L \bullet \nu)|^2 \Big) \, \mathrm{d}x \tag{7}$$

with Δ^{-1} meaning the inverse of the homogeneous Dirichlet boundary-value problem for the Laplacean defined as a map $\Delta : H^1_0(\Omega;\mathbb{R}^{d+1}) \to H^{-1}(\Omega;\mathbb{R}^{d+1})$.

The value of the internal parameter may influence the magnetization of the system and vice versa and, on the other hand, dissipated energy influences the temperature of the system, which, in turn, may affect the internal parameters. In order to capture all these effects, we employ the concept of generalized standard materials [10] known from continuum mechanics and couple our micromagnetic model with the entropy balance with the rate of dissipation on the right-hand side; cf. (9). Then the Young measure ν is considered to evolve quasistatically according to the minimization principle of the Gibbs energy $\mathscr{G}(t, \cdot, \lambda, \theta)$ while the dissipative variable λ is governed by the flow rule:

$$\partial\zeta(\dot\lambda) = \partial_\lambda g(t, \nu, \lambda, \theta) \tag{8}$$

with $\partial\zeta$ denoting the subdifferential of the convex functional $\zeta(\cdot)$ and similarly $\partial_\lambda g$ is the subdifferential of the convex functional $g(t, \nu, \cdot, \theta)$. In our specific choice, (8) takes the form $\partial\delta^*_S(\dot\lambda) + \epsilon|\dot\lambda|^{q-2}\dot\lambda + (\theta - \theta_{\mathrm{c}})\vec{a} \ni \varkappa\Delta^{-1}(\lambda - L \bullet \nu)$. Furthermore, we define the specific entropy s by the standard Gibbs relation for entropy, i.e. $s = -g'_\theta(t, \nu, \lambda, \theta)$, and write the entropy equation

$$\theta\dot{s} + \operatorname{div} j = \xi(\dot\lambda) = \ \text{ heat production rate}, \tag{9}$$

where j is the heat flux governed by the Fourier law

$$j = -\mathbb{K}\nabla\theta \tag{10}$$

with a heat-conductivity tensor $\mathbb{K} = \mathbb{K}(\lambda, \theta)$. In view of (5),

$$\xi(\dot\lambda) = \partial\zeta(\dot\lambda)\cdot\dot\lambda = \delta^*_S(\dot\lambda) + \epsilon|\dot\lambda|^q. \tag{11}$$

Now, since $s = -g'_\theta(t, \nu, \lambda, \theta) = -g'_\theta(\lambda, \theta)$, it holds $\theta\dot{s} = -\theta g''_\theta(\lambda, \theta)\dot\theta - \theta g''_{\theta\lambda}\dot\lambda$. Using also $g''_{\theta\lambda} = \vec{a}$, we may reformulate the entropy equation (9) as the heat equation

$$c_{\mathrm{v}}(\theta)\dot\theta - \operatorname{div}(\mathbb{K}(\lambda, \theta)\nabla\theta) = \delta^*_S(\dot\lambda) + \epsilon|\dot\lambda|^q + \vec{a}\cdot\theta\dot\lambda \quad \text{ with } \ c_{\mathrm{v}}(\theta) = -\theta g''_\theta(\theta), \tag{12}$$

where c_{v} is the specific heat capacity.

Altogether, we can formulate our problem for unknowns θ, ν, and λ which was first set and analyzed in

[3] as

$$\left.\begin{aligned}&\text{minimize}\quad \int_\Omega \Big(\phi\bullet\nu+(\theta-\theta_{\rm c})\vec{a}\cdot\lambda(t)-\psi_0(\theta(t))+\frac{1}{2}m\cdot\nabla u_m\\&\qquad\qquad -h(t)\cdot m+\tfrac{\varkappa}{2}\big|\nabla\Delta^{-1}(\lambda(t)-L\bullet\nu)\big|^2\Big)\,{\rm d}x\\&\text{subject to}\quad m={\rm id}\bullet\nu\qquad\text{on }\Omega,\\&\qquad\qquad {\rm div}\big(\mu_0\nabla u_m-\chi_\Omega m\big)=0\qquad\text{on }\mathbb{R}^d,\\&\qquad\qquad \nu\in\mathscr{Y}^p(\Omega;\mathbb{R}^d),\ m\in L^p(\Omega;\mathbb{R}^d),\ u_m\in H^1(\mathbb{R}^d),\end{aligned}\right\}\ \text{for } t\in[0,T],\tag{13a}$$

$$\partial\delta_S^*(\dot\lambda)+\epsilon|\dot\lambda|^{q-2}\dot\lambda+(\theta-\theta_{\rm c})\vec{a}\ni\varkappa\Delta^{-1}({\rm div}\,\lambda-L\bullet\nu)\qquad\text{in } Q:=[0,T]\times\Omega,\tag{13b}$$

$$c_{\rm v}(\theta)\dot\theta-{\rm div}(\mathbb{K}(\lambda,\theta)\nabla\theta)=\delta_S^*(\dot\lambda)+\epsilon|\dot\lambda|^q+\vec{a}\cdot\theta\dot\lambda\qquad\text{in } Q,\tag{13c}$$

$$\big(\mathbb{K}(\lambda,\theta)\nabla\theta\big)\cdot n+b\theta=b\theta_{\rm ext}\qquad\text{on }\Sigma:=[0,T]\times\Gamma,\tag{13d}$$

where we accompanied the heat equation (9) by the Robin-type boundary conditions with n denoting the outward unit normal to the boundary Γ, with $b\in L^\infty(\Gamma)$ a phenomenological heat-transfer coefficient, and with $\theta_{\rm ext}$ an external temperature, both assumed non-negative. Eventually, we equip this system with initial conditions

$$\lambda(0,\cdot)=\lambda_0,\qquad\theta(0,\cdot)=\theta_0\qquad\text{on }\ \Omega,\tag{14}$$

Transforming (9) by the so-called enthalpy transformation, we obtain a different form of (13) simpler for the analysis. For this, let us introduce a new variable w, called enthalpy, by

$$w=\widehat{c}_{\rm v}(\theta)=\int_0^\theta c_{\rm v}(r){\rm d}r.\tag{15}$$

It is natural to assume $c_{\rm v}$ positive, hence $\widehat{c}_{\rm v}$ is, for $w\ge0$ increasing and thus invertible. Therefore, denote

$$\Theta(w):=\begin{cases}\widehat{c}_{\rm v}^{-1}(w) & \text{if } w\ge0\\ 0 & \text{if } w<0\end{cases}$$

and notice that, in the physically relevant case when $\theta\ge0$, $\theta=\Theta(w)$. Thus writing the heat flux in terms of w gives

$$\mathbb{K}(\lambda,\theta)\nabla\theta=\mathbb{K}\big(\lambda,\Theta(w)\big)\nabla\Theta(w)=\mathcal{K}(\lambda,w)\nabla w,\quad\text{ where }\ \mathcal{K}(\lambda,w):=\frac{\mathbb{K}(\lambda,\Theta(w))}{c_{\rm v}(\Theta(w))}.\tag{16}$$

Moreover, the terms $(\Theta(w(t))-\theta_{\rm c})\vec{a}\cdot\lambda(t)$ and $\psi_0(\theta(t))$ obviously do not play any role in the minimization (13a) and can be omitted. Thus we may rewrite (13) in terms of w as follows:

$$\left.\begin{aligned}&\text{minimize}\quad \int_\Omega\Big(\phi\bullet\nu+\frac{1}{2}m\cdot\nabla u_m-h(t)\cdot m+\frac{\varkappa}{2}\big|\nabla\Delta^{-1}(\lambda(t)-L\bullet\nu)\big|^2\Big)\,{\rm d}x\\&\text{subject to}\quad m={\rm id}\bullet\nu,\qquad\text{on }\Omega,\\&\qquad\qquad {\rm div}\big(\mu_0\nabla u_m-\chi_\Omega m\big)=0\qquad\text{on }\mathbb{R}^d,\\&\qquad\qquad \nu\in\mathscr{Y}^p(\Omega;\mathbb{R}^d),\ m\in L^p(\Omega;\mathbb{R}^d),\ u_m\in H^1(\mathbb{R}^d),\end{aligned}\right\}\ \text{for } t\in[0,T],\tag{17a}$$

$$\partial\delta_S^*(\dot\lambda)+\epsilon|\dot\lambda|^{q-2}\dot\lambda+\big(\Theta(w)-\theta_{\rm c}\big)\vec{a}\ni\varkappa\Delta^{-1}(\lambda-L\bullet\nu)\qquad\text{in } Q,\tag{17b}$$

$$\dot w-{\rm div}(\mathcal{K}(\lambda,w)\nabla w)=\delta_S^*(\dot\lambda)+\epsilon|\dot\lambda|^q+\vec{a}\cdot\Theta(w)\dot\lambda\qquad\text{in } Q,\tag{17c}$$

$$\big(\mathcal{K}(\lambda,w)\nabla w\big)\cdot n+b\Theta(w)=b\theta_{\rm ext}\qquad\text{on }\Sigma.\tag{17d}$$

Eventually, we complete this transformed system by the initial conditions

$$\lambda(0,\cdot)=\lambda_0, \qquad w(0,\cdot)=w_0:=\widehat{c}_{\rm v}(\theta_0) \qquad \text{on } \ \Omega, \tag{18}$$

where λ_0 is the initial phase field value, and θ_0 is the initial temperature.

Now we are ready to define a weak solution to our problem. We denote by $\mathscr{Y}^p(\Omega;\mathbb{R}^d)^{[0,T]}$ the set of time-dependent Young measures, i.e., the set of maps $[0,T]\to\mathscr{Y}^p(\Omega;\mathbb{R}^d)$. We again refer to Appendix for details on Young measures.

Definition 3.1 (Weak solution [3])**.** The triple

$$(\nu,\lambda,w)\in(\mathscr{Y}^p(\Omega;\mathbb{R}^d))^{[0,T]}\times W^{1,q}([0,T];L^q(\Omega;\mathbb{R}^{d+1}))\times L^1([0,T];W^{1,1}(\Omega))$$

such that $m=\mathrm{id}\bullet\nu\in L^2(Q;\mathbb{R}^d)$ and $L\bullet\nu\in L^2(Q;\mathbb{R}^{d+1})$ is called a weak solution to (17) if it satisfies:

1. The minimization principle: For all $\tilde\nu$ in $\mathscr{Y}^p(\Omega;\mathbb{R}^d)$ and all $t\in[0,T]$

$$\mathscr{G}(t,\nu,\lambda,\Theta(w))\le\mathscr{G}(t,\tilde\nu,\lambda,\Theta(w)). \tag{19}$$

2. The magnetostatic equation: For a.a. $t\in[0,T]$ and all $\varphi\in H^1(\mathbb{R}^d)$

$$\mu_0\int_{\mathbb{R}^d}\nabla u_m\cdot\nabla\varphi\,\mathrm{d}x=\int_\Omega m\cdot\nabla\varphi\,\mathrm{d}x. \tag{20}$$

3. The flow rule: For any $\varphi\in L^q(Q;\mathbb{R}^{d+1})$

$$\begin{aligned}\int_Q\Big((\Theta(w)-\theta_{\rm c})\vec a\cdot(\varphi-\dot\lambda)+\delta_S^*(\varphi)+\frac{\epsilon}{q}|\varphi|^q+\varkappa\nabla\Delta^{-1}(\lambda-L\bullet\nu)\cdot\nabla\Delta^{-1}(\varphi-\dot\lambda)\Big)\,\mathrm{d}x\mathrm{d}t\\ \ge\int_Q\Big(\delta_S^*(\dot\lambda)+\frac{\epsilon}{q}|\dot\lambda|^q\Big)\,\mathrm{d}x\mathrm{d}t.\end{aligned} \tag{21}$$

4. The enthalpy equation: For any $\varphi\in C^1(\bar Q)$, $\varphi(T)=0$

$$\begin{aligned}\int_Q\Big(\mathcal{K}(\lambda,w)\nabla w\cdot\nabla\varphi-w\dot\varphi\Big)\,\mathrm{d}x\mathrm{d}t+\int_\Sigma b\Theta(w)\varphi\,\mathrm{d}S\mathrm{d}t=\int_\Omega w_0\varphi(0)\,\mathrm{d}x\\ +\int_Q\Big(\delta_S^*(\dot\lambda)+\epsilon|\dot\lambda|^q+\Theta(w)\vec a\cdot\dot\lambda\Big)\varphi\,\mathrm{d}x\mathrm{d}t+\int_\Sigma b\theta_{\rm ext}\varphi\,\mathrm{d}S\mathrm{d}t.\end{aligned} \tag{22}$$

5. The initial conditions in (18): $\nu(0,\cdot)=\nu_0$ and $\lambda(0,\cdot)=\lambda_0$.

Data qualifications:
The following the data qualification are needed in [3] to prove the existence of weak solutions; cf. [3]:

isothermal part of the anisotropy energy: $\phi\in C(\mathbb{R}^d)$ and

$$\exists c_1^A,c_2^A>0,\ p>4:\quad c_1^A(1+|\cdot|^p)\le\phi(\cdot)\le c_2^A(1+|\cdot|^p), \tag{23a}$$

dissipation function: $\delta_S^*\in C(\mathbb{R}^{d+1})$ positively homogeneous, and

$$\exists c_{1,D},c_{2,D}>0:\quad c_{1,D}(|\cdot|)\le\delta_S^*(\cdot)\le c_{2,D}(|\cdot|), \tag{23b}$$

external magnetic field:

$$h \in C^1([0,T];L^2(\Omega;\mathbb{R}^d)), \tag{23c}$$

specific heat capacity: $c_{\rm v} \in C(\mathbb{R})$ and, with q from (5),

$$\exists c_{1,\theta}, c_{2,\theta} > 0,\ \omega_1 \geq \omega \geq q',\ c_{1,\theta}(1{+}\theta)^{\omega-1} \leq c_{\rm v}(\theta) \leq c_{2,\theta}(1{+}\theta)^{\omega_1-1}, \tag{23d}$$

heat conduction tensor: $\mathcal{K} \in C(\mathbb{R}^{d+1}\times\mathbb{R};\mathbb{R}^{d\times d})$ and

$$\exists C_K, \kappa_0 > 0\ \forall \chi \in \mathbb{R}^d : \mathcal{K}(\cdot,\cdot) \leq C_K,\quad \chi^{\rm T}\mathcal{K}(\cdot,\cdot)\chi \geq \kappa_0|\chi|^2, \tag{23e}$$

external temperature:

$$\theta_{\rm ext} \in L^1(\Sigma),\quad \theta_{\rm ext} \geq 0,\quad \text{and}\quad b \in L^\infty(\Sigma),\quad b \geq 0, \tag{23f}$$

initial conditions:

$$\nu_0 \in \mathscr{Y}^p(\Omega;\mathbb{R}^d) \text{ solving (19)},\quad \lambda_0 \in L^q(\Omega;\mathbb{R}^{d+1}),\quad w_0 = \widehat{c}_{\rm v}(\theta_0) \in L^1(\Omega) \text{ with } \theta_0 \geq 0. \tag{23g}$$

The following theorem is proved in [3].

Theorem 3.1. Let (23) hold. Then at least one weak solution (ν,λ,w) to the problem (17) in accord with Definition 3.1 does exist. Moreover, some of these solutions satisfies also

$$w \in L^r([0,T];W^{1,r}(\Omega)) \cap W^{1,1}(I;W^{1,\infty}(\Omega)^*) \qquad \text{with } 1 \leq r < \frac{d+2}{d+1}. \tag{24}$$

The proof of the Theorem 3.1 in [3] exploits the following time-discrete approximations which also create basis for our fully discrete solution. Given $T>0$ and $T/\tau \in \mathbb{N}$ we call the triple $(\nu_\tau^k,\lambda_\tau^k,w_\tau^k) \in \mathscr{Y}^p(\Omega;\mathbb{R}^d)\times L^{2q}(\Omega;\mathbb{R}^{d+1})\times H^1(\Omega)$ the *discrete weak solution* of (17) subject to boundary condition (17d) at time-level k, $k=1\dots,T/\tau$, if it satisfies:

1. The time-incremental **minimization problem** with given λ_τ^{k-1} and w_τ^{k-1}:

$$\left.\begin{array}{l}\text{Minimize}\quad \mathscr{G}(k\tau,\nu,\lambda,\Theta(w_\tau^{k-1})) + \tau\displaystyle\int_\Omega \Big(|\lambda|^{2q} + \delta_S^*\Big(\frac{\lambda-\lambda_\tau^{k-1}}{\tau}\Big) + \frac{\epsilon}{q}\Big|\frac{\lambda-\lambda_\tau^{k-1}}{\tau}\Big|^q\Big)\,{\rm d}x \\ \text{subject to}\quad (\nu,\lambda) \in \mathscr{Y}^p(\Omega;\mathbb{R}^d)\times L^{2q}(\Omega;\mathbb{R}^{d+1}).\end{array}\right\} \tag{25a}$$

   with $\mathscr{G}$ from (7).

2. The **Poisson problem**: For all $\varphi \in H^1(\mathbb{R}^d)$

$$\int_{\mathbb{R}^d} \nabla u_{m_\tau^k}\cdot\nabla\varphi\,{\rm d}x = \int_\Omega m_\tau^k\cdot\nabla\varphi\,{\rm d}x \qquad \text{with}\quad m_\tau^k = {\rm id}\bullet\nu_\tau^k. \tag{25b}$$

3. The **enthalpy equation**: For all $\varphi \in H^1(\Omega)$

$$\begin{aligned}\int_\Omega \Big(\frac{w_\tau^k - w_\tau^{k-1}}{\tau}\varphi + \mathcal{K}(\lambda_\tau^k,w_\tau^k)\nabla w_\tau^k\cdot\nabla\varphi\Big)\,{\rm d}x + \int_\Gamma b_\tau^k\Theta(w_\tau^k)\varphi\,{\rm d}S = \int_\Gamma b_\tau^k\theta_{{\rm ext},\tau}^k\varphi\,{\rm d}S \\ + \int_\Omega \Big(\delta_S^*\Big(\frac{\lambda_\tau^k-\lambda_\tau^{k-1}}{\tau}\Big) + \epsilon\Big|\frac{\lambda_\tau^k-\lambda_\tau^{k-1}}{\tau}\Big|^q\Theta(w_\tau^k)\vec{a}\cdot\frac{\lambda^k-\lambda^{k-1}}{\tau}\Big)\varphi\,{\rm d}x.\end{aligned} \tag{25c}$$

4. For $k=0$ the **initial conditions** in the following sense

$$\nu_\tau^0=\nu_0,\qquad \lambda_\tau^0=\lambda_{0,\tau},\qquad w_\tau^0=w_{0,\tau}\quad \text{ on } \Omega. \tag{25d}$$

In (25d), we denoted by $\lambda_{0,\tau}\in L^{2q}(\Omega;\mathbb{R}^{d+1})$ and $w_{0,\tau}\in L^2(\Omega)$ respectively suitable approximation of the original initial conditions $\lambda_0\in L^q(\Omega;\mathbb{R}^{d+1})$ and $w_0\in L^1(\Omega)$ such that

$$\lambda_{0,\tau}\to\lambda_0 \ \text{ strongly in } L^q(\Omega;\mathbb{R}^{d+1}), \text{ and } \ \|\lambda_{0,\tau}\|_{L^{2q}(\Omega;\mathbb{R}^{d+1})}\le C\tau^{-1/(2q+1)}, \tag{26a}$$

$$w_{0,\tau}\to w_0 \ \text{ strongly in } L^1(\Omega), \text{ and } \ w_{0,\tau}\in L^2(\Omega). \tag{26b}$$

Moreover $\theta_{\mathrm{ext},\tau}^k\in L^2(\Gamma)$ and $b_\tau^k\in L^\infty(\Gamma)$ are defined in such a way that their piecewise constant interpolants

$$\big[\bar\theta_{\mathrm{ext},\tau},\bar b_\tau\big](t):=\big(\theta_{\mathrm{ext},\tau}^k,b_\tau^k,\big)\qquad\qquad \text{for } \ (k{-}1)\tau<t\le k\tau,\ \ k=1,...,K_\tau.$$

satisfy

$$\bar\theta_{\mathrm{ext},\tau}\to\theta_{\mathrm{ext}} \ \text{ strongly in } L^1(\Sigma) \text{ and } \ \bar b_\tau\overset{*}{\rightharpoonup} b \ \text{ weakly* in } L^\infty(\Sigma). \tag{27}$$

We introduce the notion of *piecewise affine* interpolants λ_τ and w_τ defined by

$$\big[\lambda_\tau,w_\tau\big](t):=\frac{t-(k{-}1)\tau}{\tau}\big(\lambda_\tau^k,w_\tau^k\big)+\frac{k\tau-t}{\tau}\big(\lambda_\tau^{k-1},w_\tau^{k-1}\big)\qquad \text{for } \ t\in[(k{-}1)\tau,k\tau]$$

with $k=1,...,T/\tau$. In addition, we define the backward *piecewise constant interpolants* $\bar\nu_\tau$, $\bar\lambda_\tau$, and $\bar w_\tau$ by

$$\big[\bar\nu_\tau,\bar\lambda_\tau,\bar w_\tau\big](t):=\big(\nu_\tau^k,\lambda_\tau^k,w_\tau^k\big)\qquad\qquad \text{for } \ (k{-}1)\tau<t\le k\tau,\ \ k=1,...,T/\tau. \tag{28}$$

Finally, we also need the piecewise constant interpolants of delayed enthalpy and magnetization $\underline{w}_\tau$, $\underline{m}_\tau$ defined by

$$[\underline{w}_\tau(t),\underline{m}_\tau(t)]:=[w_\tau^{k-1},\mathrm{id}\bullet\nu_\tau^{k-1}]\qquad\qquad \text{for } \ (k{-}1)\tau<t\le k\tau,\ \ k=1,...,T/\tau. \tag{29}$$

3.1 Energetics

In this section we summarize some basic energetic estimates available for our model. First we define the purely magnetic part of the Gibbs free energy $\mathfrak{G}$ as

$$\mathfrak{G}(t,\nu,\lambda):=\int_\Omega \phi\bullet\nu-h(t)\cdot m\,\mathrm{d}x+\int_{\mathbb{R}^d}\frac12|\nabla u_m|^2\,\mathrm{d}x+\frac{\varkappa}{2}\big\|\lambda-L\bullet\nu\big\|^2_{H^{-1}(\Omega;\mathbb{R}^{d+1})}. \tag{30}$$

The purely magnetic part of the Gibbs energy satisfies (see [3, Formula (4.19)]) the following energy inequality

$$\mathfrak{G}(t_\ell,\bar\nu_\tau(t_\ell),\bar\lambda_\tau(t_\ell))\le\mathfrak{G}(0,\bar\nu_\tau(0),\bar\lambda_\tau(0))+\int_0^{t_\ell}\Big(\int_\Omega\dot h_\tau\cdot\bar m_\tau\mathrm{d}x+\varkappa\big\langle\!\big\langle\bar\lambda_\tau-L\bullet\bar\nu_\tau,\dot\lambda_\tau\big\rangle\!\big\rangle\Big)\mathrm{d}t \tag{31}$$

with $t_\ell=\ell\tau$.

As $(\nu_\tau^k,\lambda_\tau^k)$ is a minimizer of (25a), the partial sub-differential of the cost functional with respect to λ has to be zero at λ_τ^k. This condition holds at each time level and, thus, summing up for $k=0,\dots,\ell$ gives

$$\begin{aligned}\int_0^{t_\ell}\!\!\int_\Omega\Big(\delta_S^*(\dot\lambda_\tau)+\frac{\epsilon}{q}|\dot\lambda_\tau|^q\Big)\mathrm{d}x\mathrm{d}t\le\int_0^{t_\ell}\!\!\Big(&\varkappa\big\langle\!\big\langle\bar\lambda_\tau{-}L\bullet\bar\nu_\tau,v_\tau{-}\dot\lambda_\tau\big\rangle\!\big\rangle\\&+\int_\Omega\Big(\big(\Theta(\underline{w}_\tau)-\theta_{\mathrm{c}}\big)\vec a\cdot(v_\tau{-}\dot\lambda_\tau)+2q\tau|\bar\lambda_\tau|^{2q-2}\bar\lambda_\tau(v_\tau{-}\dot\lambda_\tau)+\delta_S^*(v_\tau)+\frac{\epsilon}{q}|v_\tau|^q\Big)\mathrm{d}x\Big)\mathrm{d}t,\end{aligned} \tag{32}$$

where v_τ is an arbitrary test function such that $v_\tau(\cdot,x)$ is piecewise constant on the intervals $(t_{j-1},t_j]$ and $v_\tau(t_j,\cdot)\in L^{2q}(\Omega;\mathbb{R}^{d+1})$ for every j.

Hence, for $v_\tau = 0$ we get the energy balance of the thermal part of the Gibbs energy, namely

$$\int_0^{t_\ell}\int_\Omega \Big(\delta_S^*(\dot\lambda_\tau)+\frac{\epsilon}{q}|\dot\lambda_\tau|^q\Big)\mathrm{d}x\mathrm{d}t \le \int_0^{t_\ell}\Big(-\varkappa\langle\!\langle \bar\lambda_\tau - L\bullet\bar\nu_\tau, \dot\lambda_\tau\rangle\!\rangle - \int_\Omega \big(\Theta(\underline{w}_\tau)-\theta_{\mathrm{c}}\big)\vec a\cdot\dot\lambda_\tau + 2q\tau|\bar\lambda_\tau|^{2q-2}\bar\lambda_\tau\dot\lambda_\tau\Big)\mathrm{d}t\ . \tag{33}$$

This inequality couples the dissipated energy and temperature evolution.

4 Numerical approximations and computational examples

Dealing with a numerical solution, we have to find suitable spatial approximations for ν, u_m, w, and λ in each time step. In our numerical method, we require that (4) is satisfied which means that knowing the Young measure ν we can easily calculate the momenta λ. We present a spatial discretization of involved quantities in each time step.

The domain Ω of the ferromagnetic body is discretized by a regular triangulation $\mathcal{T}_\ell$ in triangles (in 2D) or in tetrahedra (in 3D) for $\ell\in\mathbb{N}$ which will be called elements. The triangulations are nested, i.e., that $\mathcal{T}_\ell\subset\mathcal{T}_{\ell+1}$, so that the discretizations are finer as ℓ increases. Let us now describe the approximation.

Young measure. Young measures are parametrized (by $x\in\Omega$) probability measures supported on $\mathbb{R}^d$. Hence, we need to handle their discretization in Ω as well as in $\mathbb{R}^d$. Our aim is to approximate a general Young measure by a convex combination of a finite number of Dirac measures (atoms) supported on $\mathbb{R}^d$ such that this convex combination is elementwise constant. Let us now describe a rigorous procedure how to achieve this goal. We first omit the time discretization parameter τ and discuss the discretization of the Young measure in Ω. In order to approximate a Young measure ν, we follow [7, 20] and define for $z\in L^\infty(\Omega)\otimes C^p(\mathbb{R}^d)$ the following projection operator ($\mathcal{L}^d$ denotes the d-dimensional Lebesgue measure)

$$[\Pi_\ell^1 z](x,s) = \frac{1}{\mathcal{L}^d(\triangle)}\int_\triangle z(\tilde x,s)\,\mathrm{d}\tilde x \quad \text{if } x\in\triangle\in\mathcal{T}_\ell\ .$$

Notice that Π_ℓ^1 is elementwise constant in the x-variable. We now turn to a discretization of $\mathbb{R}^d$ in terms of large cubes in $\mathbb{R}^d$, i.e., for $\alpha\in\mathbb{N}$ we consider a cube $B_\alpha := [-\alpha,\alpha]^d$ (i.e. we call it "a cube" even if $d=2$) which is discretized into $(2\alpha/n)^d$ smaller cubes with the edge length $2\alpha/n$ for some $n\in\mathbb{N}$. Corners of small cubes are called nodal points. We define Q_1 elements on the cube $B_\alpha\in\mathbb{R}^d$ which consist of tensorial products of affine functions in each spatial variable of $\mathbb{R}^d$. In this way, we find basis functions $f_i : B_\alpha\to\mathbb{R}$ for $i=1,\dots,(n+1)^d$ such that $f_i\ge 0$ and $\sum_{i=1}^{(n+1)^d} f_i(s)=1$ for all $s\in\mathbb{R}^d$. Moreover, if s_j is the j-th nodal point then $f_i(s_j)=\delta_{ij}$, where δ_{ij} is the Kronecker symbol. Further, each f_i can be continuously extended to $\mathbb{R}^d\setminus B_\alpha$ and such an extended function can even vanish at infinity, i.e., it belongs to $C_0(\mathbb{R}^d)$. This construction defines a projector $L^\infty(\Omega)\otimes C^p(\mathbb{R}^d)\to L^\infty(\Omega)\otimes C^p(\mathbb{R}^d)$ as

$$[\Pi_{\alpha,n}^2 z](x,s) := \sum_{i=1}^{(n+1)^d} z(x,s_i)f_i(s)\ .$$

Finally, we define $\Pi_{\ell,\alpha,n} := \Pi_\ell^1\circ\Pi_{\alpha,n}^2$, so that

$$[\Pi_{\ell,\alpha,n} z](x,s) := \frac{1}{\mathcal{L}^n(\triangle)}\sum_{i=1}^{(n+1)^d}\int_\triangle z(\tilde x,s_i)v_i(s)\,\mathrm{d}\tilde x \quad \text{if } x\in\triangle\in\mathcal{T}_\ell\ .$$

If we now take $\nu\in\mathscr{Y}^p(\Omega;\mathbb{R}^d)$ and denote $l:=(\ell,\alpha,n)$ we calculate

$$\int_\Omega\int_{\mathbb{R}^d}[\Pi_l z](x,s)\nu_x(\mathrm{d}s)\,\mathrm{d}x = \int_\Omega\int_{\mathbb{R}^d} z(x,s)[\nu_l]_x(\mathrm{d}s)\,\mathrm{d}x\ , \tag{34}$$

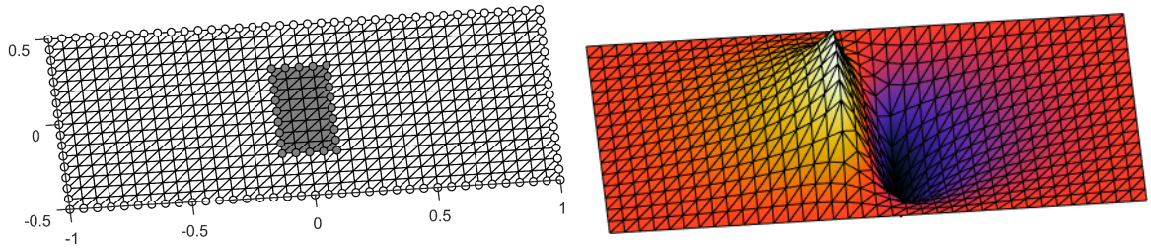

Figure 1: Example of the outer triangulation $\hat{\mathcal{T}}$ containing the magnet body triangulation $\mathcal{T}$ (in gray) is shown in the left. The right part displays an example of the magnetostatic potential u_m approximated as the scalar nodal and elementwise linear function (P1 elements function) satisfying zero Dirichlet condition in the boundary nodes of $\hat{\mathcal{T}}$.

where for $x \in \Omega$

$$[\nu_l]_x := \sum_{i=1}^{(n+1)^d} \xi_{i,l}(x)\delta_{s_i} \ , \tag{35}$$

with

$$\xi_{i,l}(x) := \frac{1}{\mathcal{L}^d(\triangle)} \int_{\triangle} \int_{\mathbb{R}^d} f_i(s)\nu_x(ds)\,\mathrm{d}x \ , \ x \in \triangle \in \mathcal{T}_\ell \ .$$

Let us denote the subset of Young measures from $\mathscr{Y}^p(\Omega;\mathbb{R}^d)$ which are in the form of (35) by $\mathscr{Y}_l^p(\Omega;\mathbb{R}^d)$. Notice that $\xi_{i,l} \geq 0$ and that $\sum_{i=1}^{(n+1)^d} \xi_{i,l} = 1$. Hence, the projector Π_l corresponds to approximation of ν by a spatially piecewise constant Young measure which can be written as a convex combination of Dirac measures (atoms). We refer to [27] for a thorough description of various kinds of Young measure approximations. In order to indicate that the measure is time-dependent we write in the k-th time-step

$$[\nu_{l,\tau}^k]_x := \sum_{i=1}^{(n+1)^d} \xi_{i,l,\tau}^k(x)\delta_{s_i} \ .$$

Magnetostatic potential. Following [6], we simplify the calculation of the reduced Maxwell system in magnetostatics by assuming that the magnetostatic potential u vanishes outside a large bounded domain $\hat{\Omega} \supset \Omega$. Hence, given $m \in L^p(\Omega;\mathbb{R}^d)$, we solve the Poisson problem $\mathrm{div}(\mu_0 \nabla u_m) = \mathrm{div}(\chi_\Omega m)$ on $\hat{\Omega}$ with homogeneous Dirichlet boundary condition $u_m = 0$ on $\partial\hat{\Omega}$. The set $\hat{\Omega}$ is discretized by an outer triangulation $\hat{\mathcal{T}}_\ell$ that contains the triangulation $\mathcal{T}_\ell$ of the ferromagnetic magnetic body. Then, the magnetostatic potential

$$u_{m_{l,\tau}^k} \in P_0^1(\hat{\mathcal{T}}_\ell) \tag{36}$$

in the k-th time-step is approximated in the space $P_0^1(\hat{\mathcal{T}}_\ell)$ of scalar nodal and elementwise linear functions defined on the triangulation $\hat{\mathcal{T}}_\ell$ and satisfying zero Dirichlet boundary conditions on the triangulation boundary $\partial\hat{\mathcal{T}}_\ell$. For illustration, see Figure 1. The magnetization vector

$$m_{l,\tau}^k \in P^0(\mathcal{T}_\ell)^d \tag{37}$$

in the k-th time-step is approximated in the space $P^0(\mathcal{T}_\ell)^d$ of vector and elementwise constant functions. Another numerical approaches to solutions of magnetostatics using e.g. BEM are also available [1].

Enthalpy. The enthalpy

$$w_{\ell,\tau}^k \in P^1(\mathcal{T}_\ell) \tag{38}$$

in the k-th time-step is approximated in the space $P^1(\mathcal{T}_\ell)$ of scalar nodal and elementwise linear functions.

Having time and spatial discretizations we can set up an algorithm to solve the problem which is just (25) with additional spatial discretization. Finally, we apply the spatial discretization just described and we

arrive at the following problem.

Given spatially discretized boundary condition (17d) and $k = 1, \dots, T/\tau$ we solve:

1. The minimization problem with given $w_{\ell,\tau}^{k-1} \in P^1(\mathcal{T}_\ell)^d$ with $\lambda_{l,\tau}^{k-1} := L \bullet \nu_{l,\tau}^{k-1}$:

$$\left.\begin{aligned} &\text{Minimize} \quad \mathscr{G}(k\tau, \nu, \lambda, \Theta(w_{\ell,\tau}^{k-1})) + \tau \int_\Omega \left(|\lambda|^{2q} + \delta_S^*\Big(\frac{\lambda - \lambda_{l,\tau}^{k-1}}{\tau}\Big) + \frac{\epsilon}{q}\Big|\frac{\lambda - \lambda_{l,\tau}^{k-1}}{\tau}\Big|^q \right) \mathrm{d}x \\ &\text{subject to} \quad \nu \in \mathscr{Y}_l^p(\Omega; \mathbb{R}^d) \ , \ \lambda := L \bullet \nu \end{aligned}\right\} \tag{39a}$$

   with $\mathscr{G}$ from (7).

2. The Poisson problem: For all $v \in P_0^1(\hat{\mathcal{T}}_\ell)$

$$\mu_0 \int_{\mathbb{R}^d} \nabla u_{m_{l,\tau}^k} \cdot \nabla \varphi \, \mathrm{d}x = \int_\Omega m_{l,\tau}^k \cdot \nabla \varphi \, \mathrm{d}x \qquad \text{with} \quad m_{l,\tau}^k = \mathrm{id} \bullet \nu_{l,\tau}^k. \tag{39b}$$

3. The enthalpy equation: For all $\varphi \in P^1(\mathcal{T}_\ell)$

$$\begin{aligned} \int_\Omega \left(\frac{w_{\ell,\tau}^k - w_{\ell,\tau}^{k-1}}{\tau} \varphi + \mathcal{K}(\lambda_{l,\tau}^k, w_{\ell,\tau}^k) \nabla w_{\ell,\tau}^k \cdot \nabla \varphi \right) \mathrm{d}x + \int_\Gamma b\Theta(w_{\ell,\tau}^k) \varphi \, \mathrm{d}S = \int_\Gamma b\theta_{\mathrm{ext},\tau}^k \varphi \, \mathrm{d}S \\ + \int_\Omega \left(\delta_S^*\Big(\frac{\lambda_{l,\tau}^k - \lambda_{l,\tau}^{k-1}}{\tau}\Big) + \epsilon \Big|\frac{\lambda_{l,\tau}^k - \lambda_{l,\tau}^{k-1}}{\tau}\Big|^q + \Theta(w_{\ell,\tau}^k) \vec{a} \cdot \frac{\lambda_{l,\tau}^k - \lambda_{l,\tau}^{k-1}}{\tau} \right) \varphi \, \mathrm{d}x. \end{aligned} \tag{39c}$$

4. For $k = 0$ the initial conditions:

$$\lambda_{l,\tau}^0 = \lambda_{0,l}, \qquad w_{\ell,\tau}^0 = w_{0,\ell} \quad \text{on } \Omega \ , \tag{39d}$$

where $\lambda_{0,\ell} = L \bullet \nu_{0,\ell}$ is calculated via (34) and $w_{0,\ell}$ is a piecewise affine approximation of w_0. There is no initial condition for $\lambda_{\ell,\tau}^0$ as it is now fully determined by $\nu_{0,\ell}$.

In computations, several simplifications were taken to account. First of all, we assume

$$d = 2, \qquad q = 2. \tag{40}$$

In view of (4), the macroscopic magnetization m is elementwise constant and it is the first moment of ν_l. As the anisotropy energy density is minimized for a given temperature on a sphere in $\mathbb{R}^d$ we put the support of the Young measure ν_l on this sphere and its vicinity to decrease the number of variables in our problem. In what follows, the number of Dirac atoms in ν_l is denoted by $N \in \mathbb{N}$. It is then convenient to work in polar coordinates where r_i is the radius and φ_i the corresponding angle of the i-th atom. Hence, we have

$$m_{l,\tau}^k = \lambda_{1,l,\tau}^k = p_\tau^k \sum_{i=1}^N \xi_{i,l,\tau}^k r_i \left(\cos(\varphi_i), \sin(\varphi_i)\right), \qquad \lambda_{2,l,\tau}^k = (p_\tau^k)^2 \sum_{i=1}^N \xi_{i,l,\tau}^k r_i^2, \qquad \sum_{i=1}^N \xi_{i,l,\tau}^k = 1, \tag{41}$$

where coefficients $\xi_{i,l,\tau}^k \in [0,1], i = 1, \dots, N$, and p_τ^k depends on temperature in the following way:

$$p_\tau^k(\theta) := \begin{cases} \sqrt{(\theta_\mathrm{c} - \theta) a_0 / (2b_0)} & \text{if } \theta_\mathrm{c} > \theta, \\ p_\mathrm{par} & \text{otherwise.} \end{cases}$$

A small parameter $p_\mathrm{par} > 0$ is introduced which allows for nonzero magnetization and increase of the temperature due to the change of magnetization even in the paramagnetic mode. The number N and values

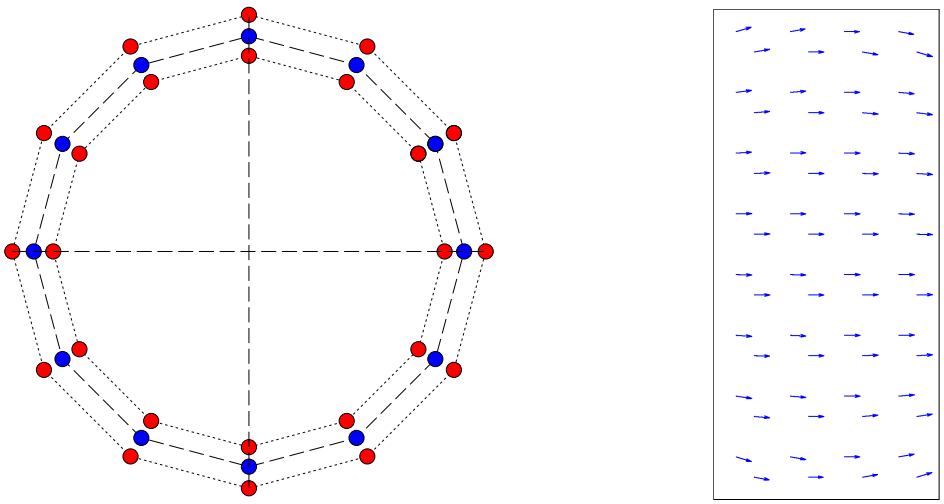

Figure 2: An example of uniformly distributed Dirac atoms on the left: Each atom is specified by its angle φ_i and radius r_i for $i = 1, \dots, N$. Here, $N = 36$ and Dirac atoms are placed on "the main sphere" with radius 1 (blue colored atoms in the color scale or dark colored atoms in the gray scale) and additional two spheres with radii $\frac{1}{1.1}$ and 1.1 (red colored atoms in the color scale or gray colored atoms in the gray scale). An example of magnetization m is displayed on the right. Each vector (arrow) corresponds to value of m in one element and its orientation is given as a convex combination of Dirac atoms multiplied by the value of p_τ^k, see (41).

of radii r_i and angles φ_i are given a priori and influence possible directions of magnetization, see Figure 2. The coefficients of the convex combinations and p_τ^k in the k-th time-step

$$\xi_{i,l,\tau}^k, p_\tau^k \in P^0(\mathcal{T}_\ell) \tag{42}$$

for all $i = 1, \dots, N$ are approximated in the space $P^0(\mathcal{T}_\ell)$ of scalar and elementwise constant functions. We assume that for $H_c, h_c > 0$

$$S := \{\lambda = (\lambda_1, \lambda_2) \in \mathbb{R}^2 \times \mathbb{R} : \ |\lambda_1| \le H_c \,\&\, |\lambda_2| \le h_c\} \ .$$

Then for $\eta \in \mathbb{R}^2 \times \mathbb{R}$

$$\delta_S^*(\eta) = \max_{\lambda \in S} \eta \cdot \lambda = H_c|\eta_1| + h_c|\eta_2| \ . \tag{43}$$

where H_c represents the coercive force of the magnetic material. Then the minimization problem (39a) can be expressed in unknown coefficients $\xi_{i,l,\tau}^k$, $i = 1, \dots, N$ only. The functional in (39a) contains a nondifferentiable norm term (43), and its evaluation requires to solve the magnetostatic potential $u_{m_{l,\tau}^k}$ from the Poisson problem (39b) with zero boundary conditions. The size of the matrix in the discretized Poisson problem equals to the number of free nodes in the triangulation $\hat{\mathcal{T}}_\ell$. After coefficients $\xi_{i,l,\tau}^k$ for $i = 1, \dots, N$ are computed, the enthalpy $w_{\ell,\tau}^k$ is solved from the enthalpy equation (39c). We consider the case

$$\mathbb{K}(\lambda, \theta) = \text{const.}, \qquad c_v(\theta) = \text{const.} \tag{44}$$

of the constant heat-conductivity $\mathbb{K}$ and the constant heat capacity c_v. Therefore, the enthalpy equation (39c) can be discretized as a linear system of equations combining stiffness and mass matrices from the discretization of a second order elliptic partial differential equation using P^1 elements. Therefore, the size of both matrices is equal to the number of all nodes in the triangulation $\mathcal{T}_\ell$.

As an example of computation, we consider a large domain $\hat{\Omega}$ and a magnet domain Ω, where

$$\hat{\Omega} = (-1, 1) \times (-\frac{1}{2}, \frac{1}{2}), \qquad \Omega = (-\frac{1}{9}, \frac{1}{9}) \times (-\frac{1}{4}, \frac{1}{4})$$

with a triangulation shown in Figure 1 (left). A Young measure was discretized using 36 Dirac measures grouped in three spherical layers as shown in Figure 2 (left).

Physical parameters were chosen to show qualitative results only and they obviously do not correspond to any realistic material. We consider

- $\phi_{\text{poles}}(m) = m_1^2$, where $m = (m_1, m_2)$ and m is measured in A/m,
- the coercive force $H_c = 100\,\text{T}$ - this value provides a hysteresis width visible in all figures,
- $h_c = 1\text{Tm/A}$
- $p_{\text{par}} = 0.1$
- the parameter[1] $\epsilon = 10^{-6}$
- the initial temperature inside magnet $\theta_0 = 1300\,\text{K}$, the Curie temperature $\theta_c = 1388\,\text{K}$ and the constant external temperature around the magnet body is $\theta_{\text{ext}} = 1100\,\text{K}$,
- the coefficient $b = 0.001\text{W/(mK)}$ in the Robin-type boundary condition, the heat conductivity coefficient ($\mathbb{I}$ stands for the identity matrix in $\mathbb{R}^{2\times 2}$) $\mathbb{K} = 100\,\mathbb{I}\text{W/m K}$ and the heat capacity $c_v = 420\text{J/(m}^3\text{K)}$,
- the coefficients in the thermo-magnetic coupling $a_0 = 1\,\text{J/(KmA}^2\text{)}$, $b_0 = 1\,\text{Jm/A}^4$,
- the uniaxial cyclic magnetic field $h(t) = 3H_c(h_x(t), 0)\text{T}$, where $t = 0, \ldots, 80$ and h_x is a cyclic periodic function with the period 10 and the amplitude 1.

As the result of the change of magnetic field inside the magnet, the magnet is heated and inside temperature increases with the boundary temperature θ_{ext} held constant over time. An increase of the temperature decreases the measure support p, and amplitudes of magnetization become smaller over time. Figures 3-5 describe average values of magnetization in x-direction and the temperature after one, two or eight cycles of external forces. With each cycle, the average temperature increases and approaches the Curie temperature. Since $\theta_{\text{ext}} < \theta_c$, the temperature inside magnet never exceeds the Curie temperature and no paramagnetic effects are observed. A similar computation can be run with two modified physical parameters, $\theta_{\text{ext}} = 1500\text{K}$, $b_0 = 0.1\text{W/(mK)}$. Then, the external temperature $\theta_{\text{ext}} > \theta_c$ allows for heating up the magnet after the Curie temperature and a higher value of b_0 speeds up the heating process, see Figure 6 for details. It should be mentioned that choosing only $N = 12$ Dirac atoms placed on "the middle sphere" does not visibly change the shapes of Figures 3-5.

The own MATLAB code is available as a package "Thermo-magnetic solver" at MATLAB Central and it can be downloaded for testing at `http://www.mathworks.com/matlabcentral/fileexchange/47878`. It utilizes the codes for an assembly of stifness and mass matrices described in [26]. The assembly is vectorized and works very fast even for fine mesh triangulations. The inbuilt MATLAB function *fmincon* (it is a part of the Optimization Toolbox that must be available) was exploited for the minimization of (25a). The function *fmincon* was run with an automatic differentiation option, which is very time consuming even on coarse mesh triangulations. In order to speed up calculations of the magnetostatic potential $u_{m_{l,\tau}^k}$ from the Poisson problem (25b), an explicit inverse of the stiffness matrix was precomputed and stored for considered coarse mesh triangulations. Geometrical and material parameters can be adjusted for own testing in the functions *start.m* and *start_magnet.m*.

[1] ϵ stands in front of λ whose units depend on a particular component. Hence, to avoid constants of value one which only carry SI units we do not specify the unit of ϵ.

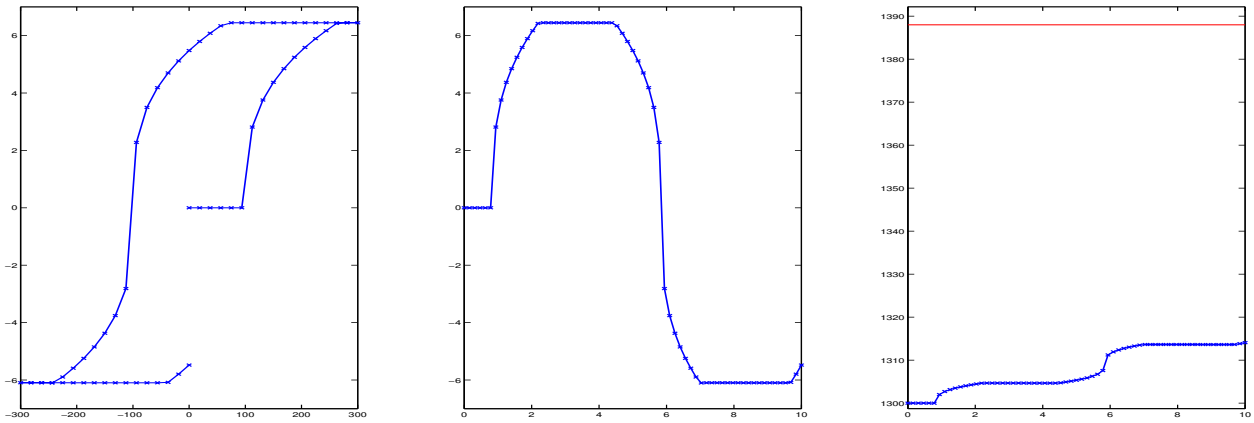

Figure 3: Average values of fields after one cycle of external forces: magnetization in x-direction versus external field (left), magnetization in x-direction versus time (middle), temperature versus time (right) never reaching the Curie temperature indicated by the red horizontal line.

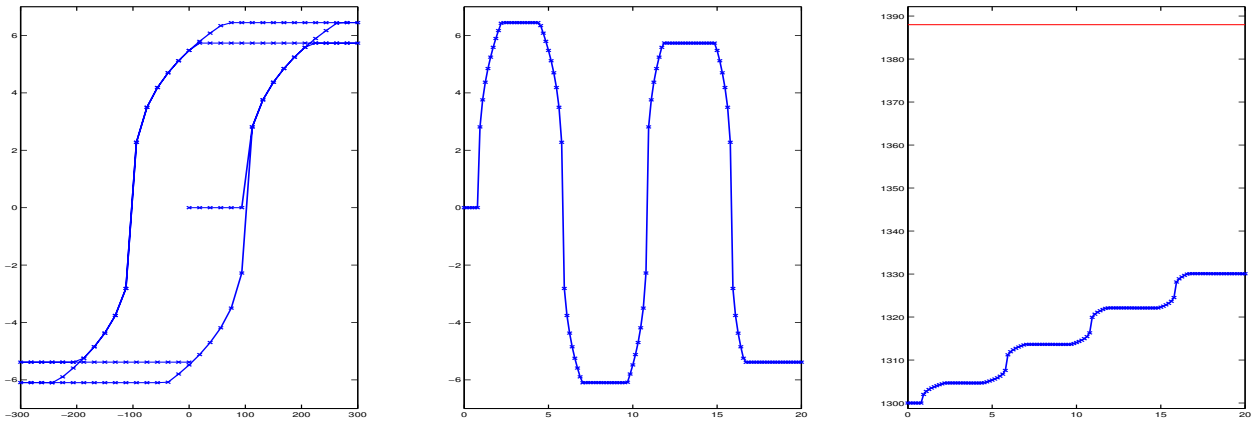

Figure 4: Average values of fields after two cycles of external forces: magnetization in x-direction versus external field (left), magnetization in x-direction versus time (middle), temperature versus time (right) never reaching the Curie temperature indicated by the red horizontal line.

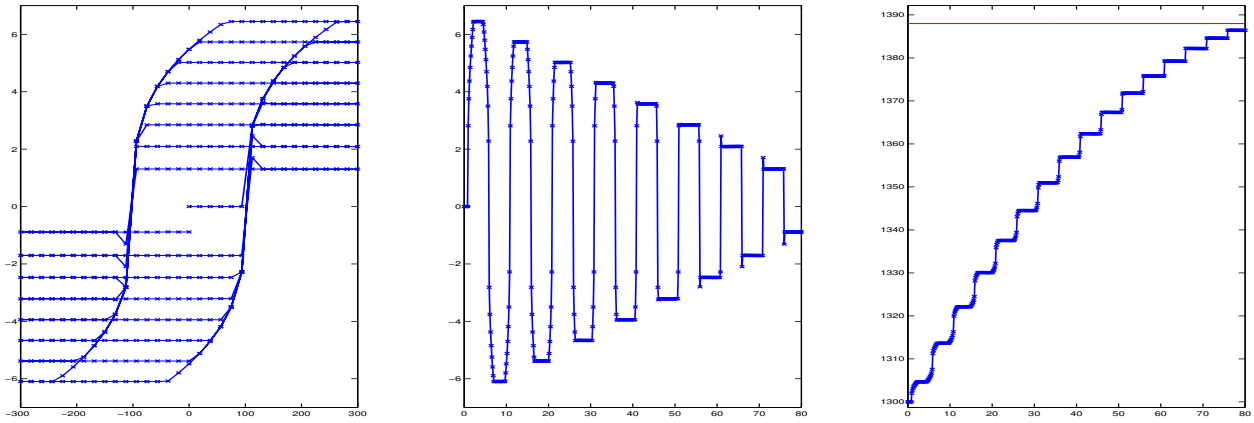

Figure 5: Average values of fields after eight cycles of external forces: magnetization in x-direction versus external field (left), magnetization in x-direction versus time (middle), temperature versus time (right)never reaching the Curie temperature indicated by the red horizontal line.

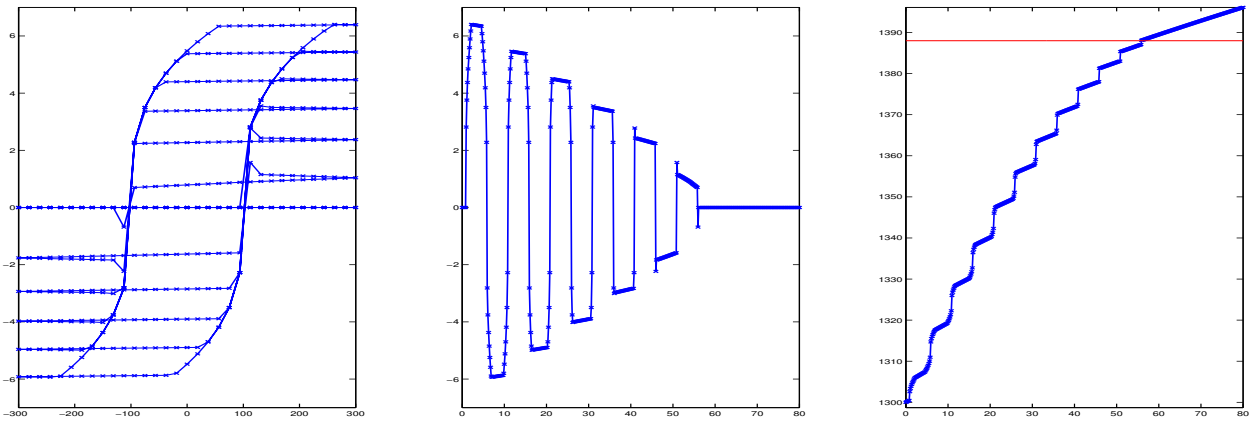

Figure 6: Average values of fields after eight cycles of external forces: magnetization in x-direction versus external field (left), magnetization in x-direction versus time (middle), temperature versus time (right) reaching and exceeding the Curie temperature indicated by the red horizontal line.

5 Concluding remarks

We tested computational performance of the model from [3] on two-dimensional examples. In spite of a few simplifications (in particular, setting $\varkappa := +\infty$), computational results are in qualitative agreement with physically observed phenomena. Interested readers are invited to perform their own numerical tests with a MATLAB code available on the web-page mentioned above. Adaptive approaches similar to the one in [7, 14] could be used to allow for much finer discretizations of Young measure support and, as a consequence, for more accurate numerical approximations. Investigations of a convergence of the above scheme as well as verification of discrete energy inequalities from (31) and (33) are left for our future work.

Acknowledgment: We thank anonymous referees for valuable comments and remarks which improved final exposition of our work. We also acknowledge the support by GAČR through projects 13-18652S, 16-34894L and by MŠMT ČR through project 7AMB16AT015.

6 Appendix – Young measures

The Young measures on a bounded domain $\Omega \subset \mathbb{R}^n$ are weakly* measurable mappings $x \mapsto \nu_x : \Omega \to \mathrm{rca}(\mathbb{R}^d)$ with values in probability measures; and the adjective "weakly* measurable" means that, for any $v \in C_0(\mathbb{R}^d)$, the mapping $\Omega \to \mathbb{R} : x \mapsto \langle \nu_x, v\rangle = \int_{\mathbb{R}^d} v(\lambda)\nu_x(\mathrm{d}\lambda)$ is measurable in the usual sense. Let us remind that, by the Riesz theorem, $\mathrm{rca}(\mathbb{R}^d)$, normed by the total variation, is a Banach space which is isometrically isomorphic with $C_0(\mathbb{R}^d)^*$, where $C_0(\mathbb{R}^d)$ stands for the space of all continuous functions $\mathbb{R}^d \to \mathbb{R}$ vanishing at infinity. Let us denote the set of all Young measures by $\mathscr{Y}(\Omega;\mathbb{R}^d)$. It is known that $\mathscr{Y}(\Omega;\mathbb{R}^d)$ is a convex subset of $L^\infty_{\mathrm{w}}(\Omega;\mathrm{rca}(\mathbb{R}^d)) \cong L^1(\Omega;C_0(\mathbb{R}^d))^*$, where the subscript "w" indicates the property "weakly* measurable". A classical result [32] is that, for every sequence $\{y_k\}_{k\in\mathbb{N}}$ bounded in $L^\infty(\Omega;\mathbb{R}^d)$, there exists its subsequence (denoted by the same indices for notational simplicity) and a Young measure $\nu = \{\nu_x\}_{x\in\Omega} \in \mathscr{Y}(\Omega;\mathbb{R}^d)$ such that

$$\forall f \in C_0(\mathbb{R}^d): \qquad \lim_{k\to\infty} f\circ y_k = f_\nu \qquad \text{weakly* in } L^\infty(\Omega)\ , \tag{45}$$

where $[f\circ y_k](x) = f(y_k(x))$ and

$$f_\nu(x) = \int_{\mathbb{R}^d} f(s)\nu_x(\mathrm{d}s)\ . \tag{46}$$

Let us denote by $\mathscr{Y}^\infty(\Omega;\mathbb{R}^d)$ the set of all Young measures which are created by this way, i.e. by taking all bounded sequences in $L^\infty(\Omega;\mathbb{R}^d)$. Note that (45) actually holds for any $f:\mathbb{R}^d\to\mathbb{R}$ continuous.

A generalization of this result was formulated by Schonbek [31] (cf. also [27]): if $1\le p<+\infty$: for every sequence $\{y_k\}_{k\in\mathbb{N}}$ bounded in $L^p(\Omega;\mathbb{R}^d)$ there exists its subsequence (denoted by the same indices) and a Young measure $\nu=\{\nu_x\}_{x\in\Omega}\in\mathscr{Y}(\Omega;\mathbb{R}^d)$ such that

$$\forall f\in C_p(\mathbb{R}^d):\qquad \lim_{k\to\infty} f\circ y_k=f_\nu \qquad \text{weakly in } L^1(\Omega)\ . \tag{47}$$

We say that $\{y_k\}$ generates ν if (47) holds. Here for $p\ge 1$, we recall that $C_p(\mathbb{R}^d)=\{f\in C(\mathbb{R}^d);\ f/(1+|\cdot|^p)\in C_0(\mathbb{R}^d)\}$.

Let us denote by $\mathscr{Y}^p(\Omega;\mathbb{R}^d)$ the set of all Young measures which are created by this way, i.e. by taking all bounded sequences in $L^p(\Omega;\mathbb{R}^d)$. It is well-known, however, that for any $\nu\in\mathscr{Y}^p(\Omega;\mathbb{R}^d)$ there exists a special generating sequence $\{y_k\}$ such that (47) holds even for $f\in C^p(\mathbb{R}^d)=\{y\in C(\mathbb{R}^d);\ |y|/(1+|\cdot|^p)\le C,\ C>0\}$.

References

[1] Z. Andjelic, G. Of, O. Steinbach, P. Urthaler, Boundary element methods for magnetostatic field problems: a critical view, Comput. Vis. Sci. 14 (2011), 117–130.

[2] L. Baňas, A. Prohl, M. Slodička, Modeling of thermally assisted magnetodynamics, SIAM J. Num. Anal. 47 (2008), 551–574.

[3] B. Benešová, M. Kružík, T. Roubíček, Thermodynamically-consistent mesoscopic model of the ferro/paramagnetic transition, Zeit. Angew. Math. Phys. 64 (2013), 1-28.

[4] A. Bergqvist, Magnetic vector hysteresis model with dry friction-like pinning, Physica B 233 (1997), 342–347.

[5] W.F. Brown, Jr., Magnetostatic Principles in Ferromagnetism, Springer, New York, 1966.

[6] C. Carstensen, A. Prohl, Numerical analysis of relaxed micromagnetics by penalised finite elements, Numer. Math. 90 (2001), 65-99.

[7] C. Carstensen, T. Roubíček, Numerical approximation of Young measures in non-convex variational problems, Numer. Math. 84 (2000), 395–415.

[8] R. Choksi, R.V. Kohn, Bounds on the micromagnetic energy of a uniaxial ferromagnet, Comm. Pure Appl. Math. 55 (1998), 259–289.

[9] A. DeSimone, Energy minimizers for large ferromagnetic bodies, Arch. Rat. Mech. Anal. 125 (1993), 99–143.

[10] B. Halphen, Q. S. Nguyen, Sur les materiaux standards généralisés, J. Mécanique 14 (1975), 39-63.

[11] A. Hubert, R. Schäfer, Magnetic Domains: The Analysis of Magnetic Microstructures, Springer, Berlin, 1998.

[12] R.D. James, D. Kinderlehrer, Frustration in ferromagnetic materials, Continuum Mech. Thermodyn. 2 (1990), 215–239.

[13] R.D. James, S. Müller, Internal variables and fine scale oscillations in micromagnetics, Continuum Mech. Thermodyn. 6 (1994), 291–336.

[14] M. Kružík, A. Prohl, Young measure approximation in micromagnetics, Numer. Math. 90 (2001), 291–307.

[15] M. Kružík, A. Prohl, Recent developments in the modeling, analysis, and numerics of ferromagnetism, SIAM Rev., 48 (2006), 439–483.

[16] M. Kružík, T. Roubíček, Specimen shape influence on hysteretic response of bulk ferromagnets, J. Magnetism and Magn. Mater. 256 (2003), 158-167.

[17] M. Kružík, T. Roubíček, Interactions between demagnetizing field and minor-loop development in bulk ferromagnets, J. Magnetism and Magn. Mater. 277 (2004), 192-200.

[18] L.D. Landau, E.M. Lifshitz, On theory of the dispersion of magnetic permeability of ferromagnetic bodies, Physik Z. Sowjetunion 8 (1935), 153–169.

[19] L.D. Landau, E.M. Lifshitz, Course of Theoretical Physics. vol. 8, Pergamon Press, Oxford, 1960.

[20] A.-M. Mataché, T. Roubíček, C. Schwab, Higher-order convex approximations of Young measures in optimal control, *Adv. in Comput. Math.* 19 (2003), 73–97.

[21] A. Mielke, T. Roubíček, Rate-independent model of inelastic behaviour of shape-memory alloys, Multiscale Modeling Simul. 1 (2003), 571-597.

[22] P. Pedregal, Relaxation in ferromagnetism: the rigid case, J. Nonlinear Sci. 4 (1994), 105–125.

[23] P. Pedregal, Parametrized Measures and Variational Principles, Birkhäuser, Basel, 1997.

[24] P. Pedregal, B. Yan, A Duality Method for Micromagnetics, SIAM J. Math. Anal. 41 (2010), 2431–2452.

[25] P. Podio-Guidugli, T. Roubíček, G. Tomassetti, A thermodynamically-consistent theory of the ferro/paramagnetic transition. Arch. Rat. Mech. Anal. 198 (2010), 1057-1094.

[26] T. Rahman, J. Valdman, Fast MATLAB assembly of FEM matrices in 2D and 3D: nodal elements, Applied Mathematics and Computation 219 (2013), 7151–7158.

[27] T. Roubíček, Relaxation in Optimization Theory and Variational Calculus, W. de Gruyter, Berlin, 1997.

[28] T. Roubíček, M. Kružík, Microstructure evolution model in micromagnetics. Z. Angew. Math. Phys. 55 (2004), 159–182.

[29] T. Roubíček, M. Kružík, Mesoscopic model for ferromagnets with isotropic hardening, Z. Angew. Math. Phys. 56 (2005), 107–135.

[30] T. Roubíček, G. Tomassetti, Ferromagnets with eddy currents and pinning effects: their thermodynamics and analysis, Math. Models Meth. Appl. Sci. (M3AS) 21 (2011), 29-55.

[31] M.E. Schonbek, Convergence of solutions to nonlinear dispersive equations, Comm. Partial Diff. Equations 7 (1982) 959–1000.

[32] L.C. Young, Generalized curves and the existence of an attained absolute minimum in the calculus of variations, Comptes Rendus de la Société des Sciences et des Lettres de Varsovie, Classe III 30 (1937), 212–234.